The potential to breed for genetic legacy effects in sustainable farming systems

Shanice Van Haeften[1#], Stephanie M. Brunner[1#], Eric Dinglasan[1], Edward Fabreag[1], Joseph Eyre[1], Celine Mens[1], Ben J Hayes[1], Michael Udvardi[1], Samir Alahmad[1], Mitchell Eglinton[1], Ryan McQuinn[2], Merrill Ryan[3], Sarah van der Meer[1], Millicent R. Smith[1,4]*, Lee T. Hickey[1*]

[1]Queensland Alliance for Agriculture and Food Innovation, The University of Queensland, QLD, Australia

[2]School of Science, Western Sydney University, NSW, Australia

[3]Queensland Department of Primary Industries, Warwick, QLD, Australia

[4]School of Agriculture and Food Sustainability, Faculty of Science, The University of Queensland, QLD, Australia

[#]Shanice Van Haeften and Stephanie M. Brunner contributed equally to this work.

Correspondence: Lee T. Hickey and Millicent R. Smith are co-corresponding authors.

Email: l.hickey@uq.edu.au

Email: millicent.smith@uq.edu.au

Abstract

Pulse crops provide protein-rich food, critical disease breaks in cereal rotations, and contribute to soil fertility through symbiotic nitrogen fixation. However, crop improvement programs typically only focus on individual crop performance rather than system-wide benefits. We propose a novel approach: breeding pulses and cereals to optimize rotational effects and enhance farming system sustainability in addition to crop-specific traits. In this proof-of-concept study, we evaluated how genetically diverse mungbeans influence subsequent wheat performance. A mini-core panel of 309 mungbean accessions was grown at a nitrogen depleted site, followed by a single wheat cultivar sown in the same plot locations. Remarkably, wheat yield ranged from 2.51 to 3.49 t ha^{-1} and displayed moderate broad-sense heritability (H^2: 0.42) as a trait of the proceeding mungbean genotype. This variation demonstrates untapped genetic potential for breeding mungbean varieties that enhance subsequent wheat performance. Integrated analyses of mungbean-wheat traits, soil properties, and microbiome composition revealed mechanisms underlying these rotational relationships. Haplotype mapping identified genomic regions in mungbean associated with wheat yield and quality. To explore how legacy traits could be leveraged in breeding programs, we conducted forward genetic simulations using empirically derived haplotype effects to compare strategies targeting mungbean yield, wheat yield, or both simultaneously. These simulations reveal both challenges and opportunities in breeding crops collectively for rotational benefits, offering a pathway toward more sustainable and profitable farming systems with reduced input requirements.

Introduction

Modern crop breeding programs typically aim to optimize a single species, focusing on traits that enhance yield and quality, irrespective of the preceding or subsequent crops in rotation (Bennett et al., 2012). This approach achieved remarkable success during the Green Revolution, transforming wheat and rice production through high-yielding cultivars that fed billions globally, though often requiring increased fertilizer and irrigation inputs (Evenson and Gollin, 2003). Importantly, breeding remains effective even in low-input systems, as demonstrated by continued genetic gains across diverse production environments (Voss-Fels et al., 2019). However, the global population will approach 10 billion by 2050 and agricultural systems have become increasingly reliant on external inputs (nitrogen fertilizer use has increased over 40% globally since 1990; Li et al., 2025), and is expected to increase further to feed the growing population despite the growing pressure to reduce them due to environmental and health concerns. Therefore this calls for innovative breeding strategies to accelerate genetic

gain and improve sustainability (Hickey et al., 2019). The single-crop breeding paradigm may be missing critical genetic opportunities when the farming system is holistically considered.

Emerging evidence suggests that genetic variation within crop species creates measurable effects on subsequent crops in rotation (Rose et al., 2010; Ellouze et al., 2013), yet the genetic basis of these "legacy effects" remains largely unexplored. Legacy effects occur when the genetic characteristics of one crop influence the performance of subsequent crops through persistent changes to soil conditions that carry over between growing seasons (Somenahally et al., 2018; Lilley and Kirkegaard, 2016). While the benefits of crop rotations at the cross-species level are well established, for example legumes fixing nitrogen for cereals (e.g. Zhao et al., 2022), crop rotations to break disease cycles (e.g. Kirkegaard et al., 1997), and diverse root systems improving soil structure (e.g. Yu et al., 2025), the genetic variation within species that could enhance these rotational benefits through targeted breeding remains unknown and is untapped in current breeding programs. Lilley and Kirkegaard (2016) highlight this concept, demonstrating that wheat cultivars with deeper, more extensive root systems extracted additional subsoil water but left soils drier at subsequent crop sowing, reducing predicted yield benefits when legacy effects were considered. Thus, selection for deeper root architecture within wheat breeding germplasm could lead to higher yielding wheat cultivars, but they may result in unintended negative consequences for subsequent crops. Integrating legumes into crop rotations enriches soil nitrogen through symbiotic nitrogen fixation, benefiting subsequent crops with yield increases often exceeding 10% and with substantial reductions in fertilizer requirements (Cernay et al., 2018; Zhao et al., 2022). However, the extent to which genetic variation within legume crop species could amplify these benefits remains unexplored. We hypothesize that the genetic architecture of crops directly modulates the phenotypic expression and yield of subsequent crops, creating heritable legacy effects that can be leveraged through breeding to optimize integrated farming system productivity (Fig 1). To test this, we conducted a proof-of-concept study using a wheat-based rotation system, and mungbean (*Vigna radiata*) as a preceding legume crop. Mungbean contributes to the system by fixing nitrogen and providing a disease break thereby enhancing the productivity and health of the subsequent wheat crop (Ilyas et al., 2018; Foyer, Nguyen & Lam, 2019). We evaluated how ~300 genetically diverse mungbean accessions influenced performance of a subsequent wheat crop rotation, combined with haplotype mapping to identify genomic regions influencing both direct mungbean traits and legacy effects on wheat productivity and quality. Through genetic simulations using real haplotype effects, we further evaluated the future potential of breeding

programs that systematically consider legacy traits alongside traditional performance metrics, demonstrating that such integrated approaches are not only feasible but could improve genetic gain and productivity for both crops through enhancing resource use efficiency for sustainable agriculture.

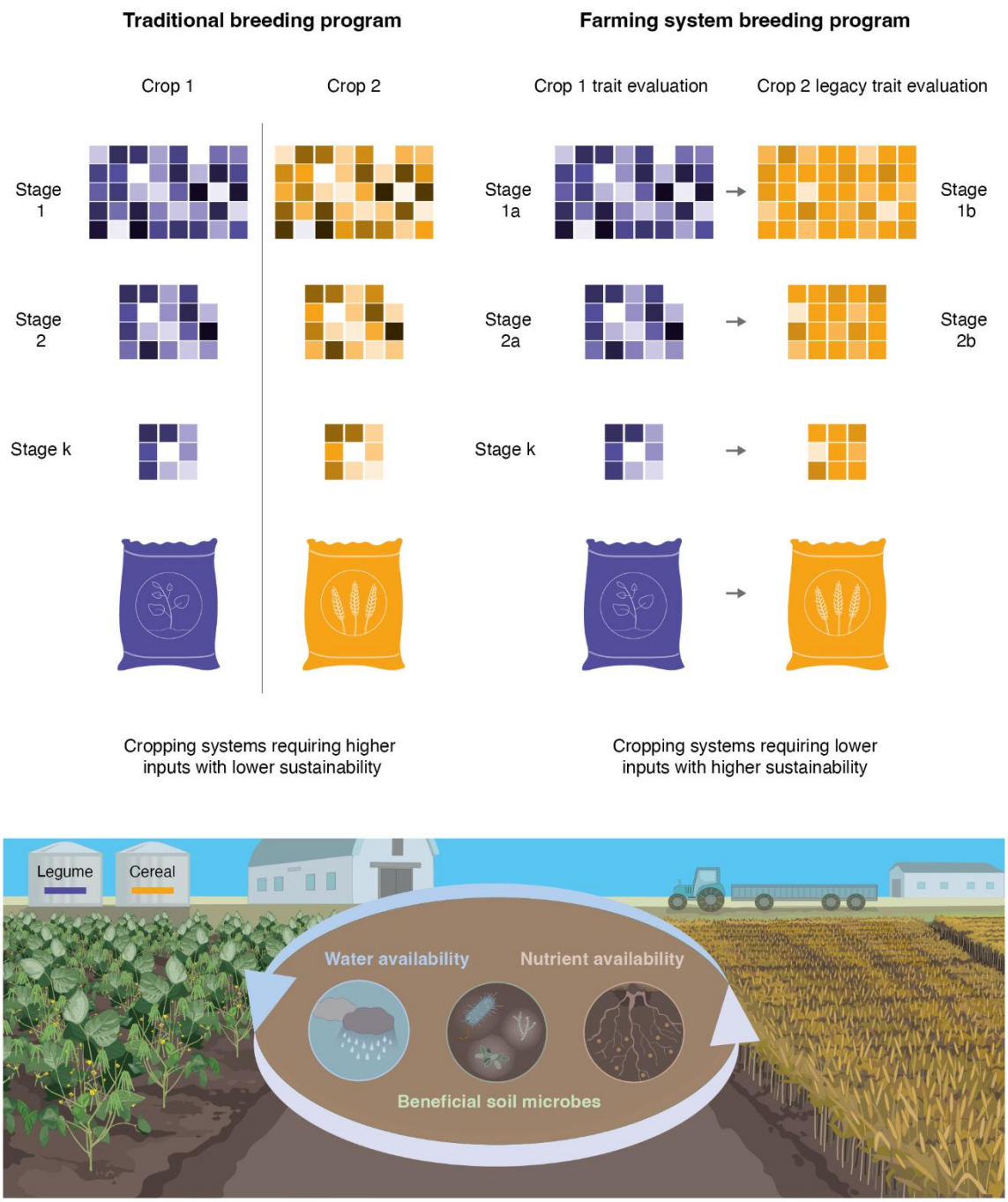

Fig 1. Conceptual framework for integrating legacy traits into farming systems breeding. *Schematic overview comparing traditional breeding approaches with a farming systems breeding strategy that could consider legacy trait selection. The traditional breeding program*

model focuses on optimising crop performance in isolation, whereas the farming systems breeding approach could also consider potential genetic effects of one crop on the next, termed legacy traits, within rotational systems. In the farming systems approach, Crop 1 undergoes evaluation for both direct performance traits and legacy effects on Crop 2 (Stage 1a), followed by assessment of Crop 2's legacy trait expression (Stage 1b), with this dual evaluation continuing through subsequent breeding stages. The lower panel illustrates the potential flow-on impact of considering legacy traits in breeding pipelines, which could enable the selection of genotypes that enhance overall system productivity through improved water-use efficiency, nutrient-use efficiency, and beneficial soil properties, including microbes. This framework represents a potential paradigm shift toward multi-crop, multi-season breeding that could support sustainable agricultural intensification while reducing input requirements.

Results

High and heritable legacy trait variation across mungbean genotypes

In the mungbean mini-core panel, substantial phenotypic variation with moderate to high broad sense heritability was observed across all measured mungbean traits (Fig. 2a; Supplementary Table 1 and 2). Mungbean yield varied 11-fold from 0.21 to 2.19 t ha^{-1}, with the check cultivar Crystal producing 1.31 t ha^{-1}. Mungbean aboveground biomass at mid canopy development showed 2.6-fold variation (151.07 to 393.31 g m^{-2}), with Crystal reaching 280.73 g m^{-2}. Vegetation index values derived from UAV-based imaging (mungbean NDRE) at 90% black pod exhibited 2.5-fold variation (0.18 to 0.45; Crystal: 0.23), indicating considerable genotypic diversity in canopy vigour and greenness. All mungbean traits exhibited high heritability (H^2 = 0.63–0.84).

To quantify legacy effects after harvest of the mungbean genotypes, we measured wheat yield for the single cultivar LongReach Raider. Wheat yield varied substantially by preceding mungbean genotype (2.52 to 3.49 t ha^{-1}), with wheat grown after mungbean cultivar Crystal yielding 3.06 t ha^{-1}. Wheat protein content varied from 7.36% to 8.48% (wheat crop grown on preceding Crystal crop: 8.14%), while wheat NDRE ranged from 0.38 to 0.43 (wheat crop grown on preceding Crystal crop: 0.41). Critically, wheat legacy traits showed moderate to high heritability (H^2 = 0.43–0.65), indicating that a substantial portion of variation in wheat performance was attributable to mungbean genotype. Several genotypes enhanced subsequent wheat yield by up to 45% relative to the commercial mungbean cultivar Crystal, while others

reduced yield by as much as 50%, underscoring the substantial impact of mungbean genetic background and growth on rotational crop productivity (Fig. 2b).

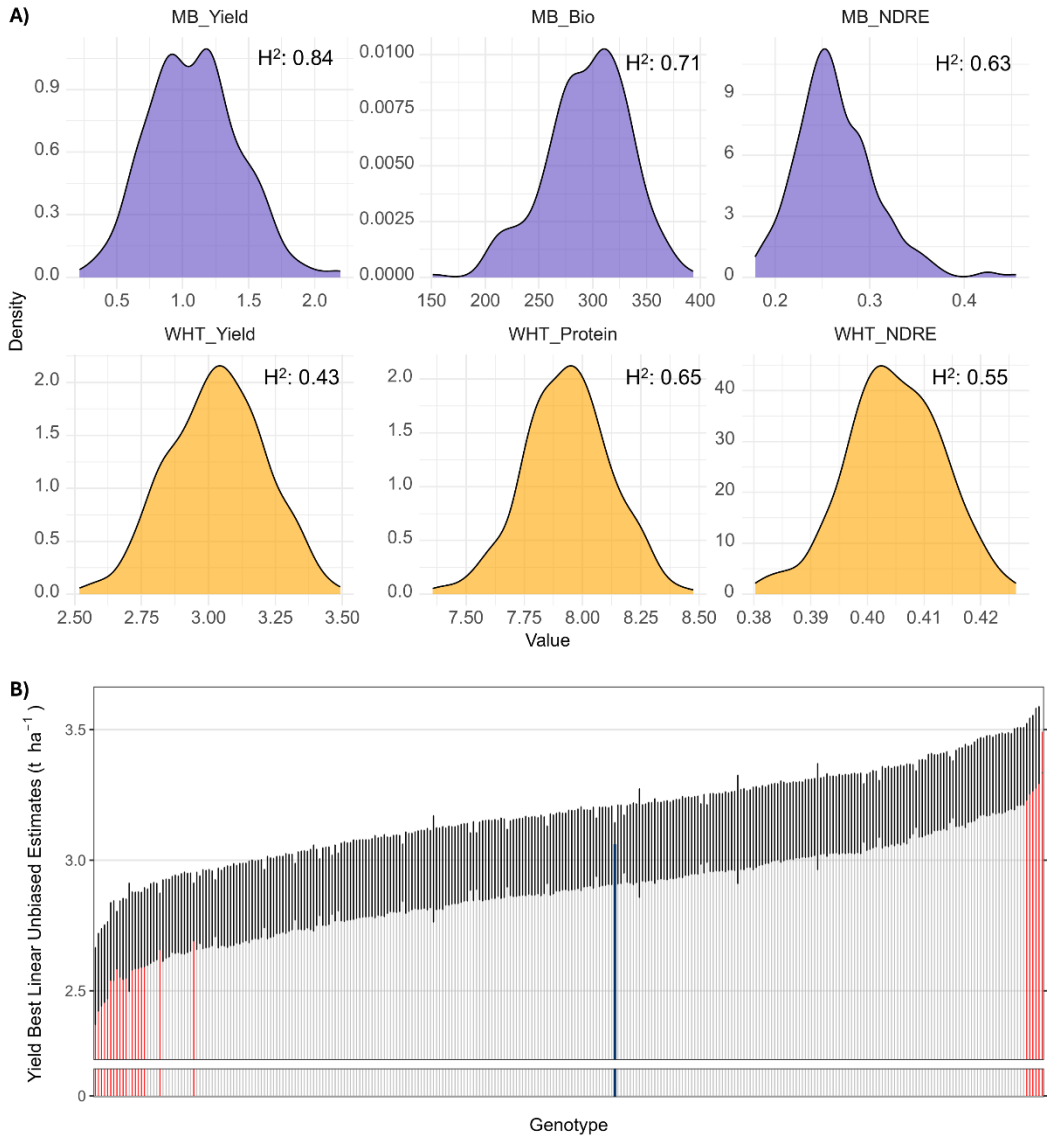

Fig 2. Genotypic variation and heritability of mungbean traits and their legacy effects on subsequent wheat yield. *a) Distribution of phenotypic values for direct mungbean physiological traits (yield, biomass, NDRE; purple) and wheat legacy traits (yield, grain protein, NDRE; orange) measured across diverse mungbean genotypes. Broad-sense heritability (H^2) estimates for each trait are indicated in the top-right corner of each panel. b) Yield performance of wheat plots, ordered by increasing yield (t ha^{-1}), reflecting legacy effects from preceding mungbean genotypes. Each bar represents the yield best linear unbiased estimates and standard error of wheat planted on individual mungbean genotype. Red bars*

denote wheat plots that have a significantly different legacy-induced yield response relative to wheat grown on the check mungbean cultivar 'Crystal' (blue).

Interactions between direct and legacy traits reveal trade-offs

Relationships between mungbean and wheat legacy traits varied in directionality and strength when evaluated across phenotypic, genetic, and haplotype levels (Fig. 3). At the phenotypic level (Fig 3a), mungbean yield showed a moderate negative correlation with wheat yield (r = −0.39, p = <0.05), suggesting potential trade-offs between mungbean productivity and subsequent crop performance. In contrast, wheat NDRE measured at flowering and wheat yield were positively correlated (r = 0.75, p = <0.05), indicating consistency among wheat physiological performance metrics. Wheat NDRE at flowering also showed a significant negative correlation with mungbean yield (r = -0.48, p = <0.05).

Genetic correlations revealed stronger associations, highlighting underlying genetic relationships not evident at the phenotypic level (Fig 3b). Mungbean NDRE at 90% black pod exhibited strong negative genetic correlations with all wheat traits (wheat yield r = −0.90; wheat protein r = −0.95; wheat NDRE r = −0.92), suggesting that genetic architecture underlying mungbean chlorophyll concentration and photosynthetic capacity captured by NDRE late in the season may be antagonistic to wheat legacy performance. Conversely, mungbean yield showed moderately low negative genetic correlation with mungbean biomass (r = -0.32) and wheat yield (r = -0.29), but a strong positive genetic correlation with wheat protein (r = 0.73). Wheat protein displayed positive genetic relationships with both wheat NDRE at flowering (r = 0.68), wheat biomass (r = 0.88) and wheat yield (r = 0.67), reinforcing coherence among wheat performance traits, as well as a strong positive genetic correlation with mungbean biomass (r = 0.88).

Haplotype-level variance correlations were uniformly positive across all mungbean and wheat traits (r = 0.28–0.78, p = <0.05), indicating that shared genomic regions contribute to trait variation across the mungbean–wheat system (Fig 3c). However, haplotype effect correlations revealed more nuanced patterns, including directional shifts between traits (Fig 3d). Mungbean yield showed strong negative haplotype effect correlations with wheat yield (r = −0.61, p = <0.05) and wheat NDRE (r = −0.77, p = <0.05), but positive associations with mungbean biomass (r = 0.60, p = <0.05) and wheat protein (r = 0.70, p = <0.05). These contrasting directions suggest trade-offs at the genome level and highlight key haplotypes that differentially influence mungbean performance and legacy benefits to wheat.

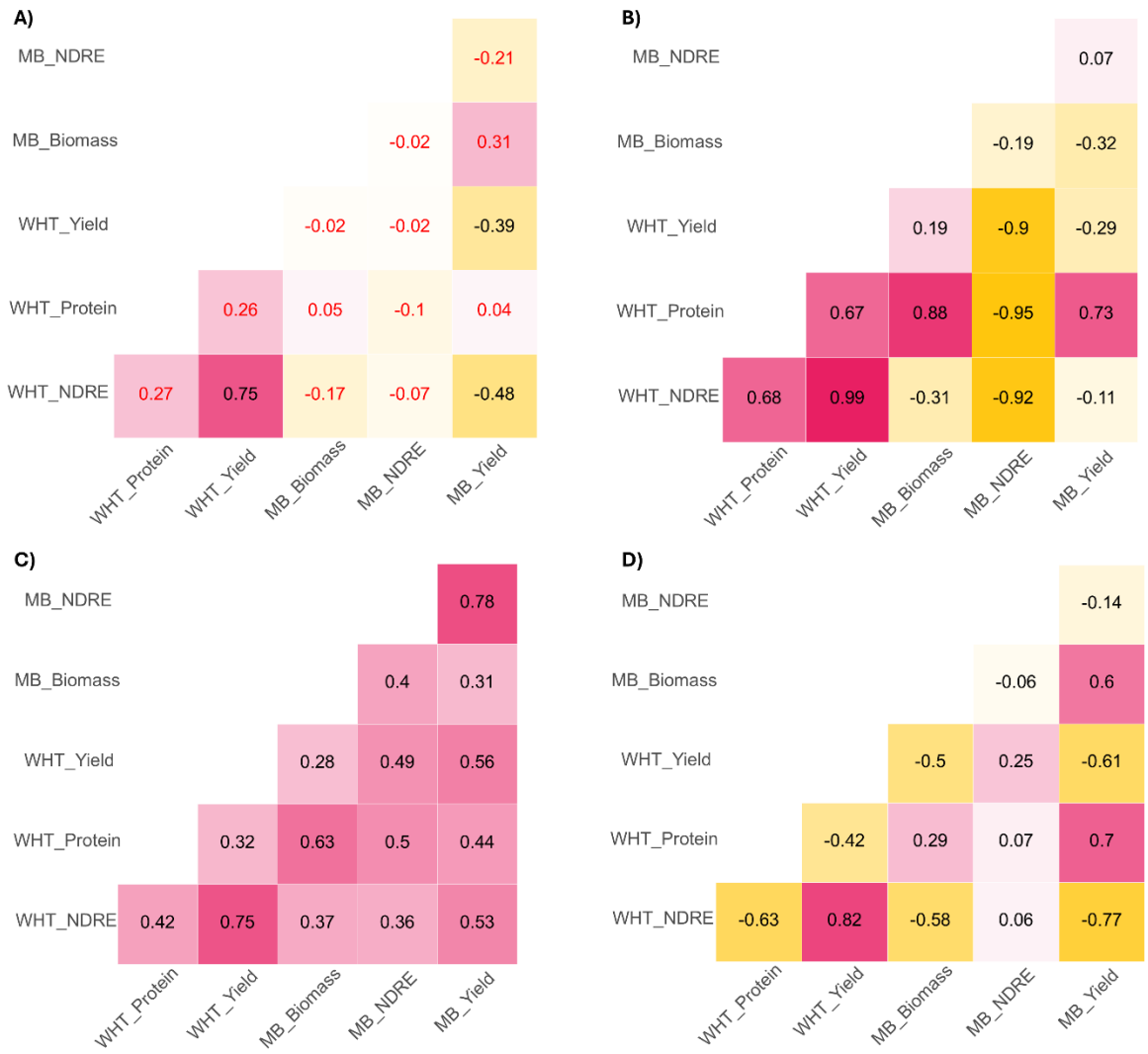

Fig 3. Correlations among mungbean and wheat legacy traits at phenotypic, genetic, and haplotype levels. *A) Phenotypic correlations (r) among mungbean and wheat legacy traits, based on BLUEs across all genotypes. B) Genetic correlations estimated from mixed-model variance components, revealing shared genetic architecture between traits. C) Correlation of haplotype-level variance across traits, reflecting the shared genomic regions contributing to trait variation. D) Correlation of haplotype effects, quantifying the concordance in direction and magnitude of haplotype influences across traits. The divergent colour key ranges from 1 (pink - positive correlation) through -1 (yellow - negative correlation). Non-significant correlations are indicated in red text.*

Following haplotype mapping, the top 12 haploblocks showing highest variance were selected and reported as most important for each trait. A total of 33 unique haploblocks were identified across all traits (Supplementary Table 3). Seventeen haploblocks were unique to single traits, with eight showing high variance for wheat legacy effects but not for any measured mungbean traits (Fig 4a and Supplementary Fig 1). Of the other 16 haploblocks all were found to have high variance for at least two traits across both wheat and mungbean. Notably, one haploblock (b000055, chr 1) was identified as high variance for all six traits across both species. Three additional haploblocks, b000160 (chr 2), b000221 (chr 3), and b000509 (chr 5), showed high variance for five of the six traits, suggesting that these genomic regions harbor loci with pleiotropic effects within mungbean, and genetically mediated legacy effects influencing wheat traits in rotation systems.

Among the top haploblocks, five were shared across mungbean yield and wheat yield (Fig. 4a), including b000022 (chr 1), b000055 (chr 1), b000221 (chr 2), b000253 (chr 2), and b000509 (chr 5), while seven high-variance haploblocks did not overlap between crops. This pattern indicates both shared and independent genetic control of direct versus legacy traits.

Functional genes associated with nitrogen fixation in legumes were positioned within five top haploblocks identified in this study (Supplementary Table 4). Interestingly, co-located genes were associated with broader root development processes, including gibberellin signalling (*MtDELLA2*), root meristem maintenance (*MtPLT1–4*), and auxin transport (*MtPIN2–4*), suggesting that root architecture may be a key mechanism underlying legacy effects.

To dissect these relationships at higher resolution, we examined two haploblocks in detail: b000055 (chr 1), the only haploblock with high variance for all six traits, and b000942 (chr 10), a haploblock with high variance for wheat yield but not ranking among the top 12 for mungbean yield. At haploblock b000055, haplotypes with the strongest positive effects for mungbean yield were associated with greater negative effects on wheat yield, consistent with the overall negative genetic correlation (Fig. 4b). This pattern illustrates the genomic basis of trade-offs between direct crop performance and legacy benefits. In contrast, block b000942 was not among the highest-variance regions for mungbean yield but nonetheless exhibited haplotype variance comparable to that observed for wheat, where it ranked among the top variance haploblocks. Importantly, this haploblock harbored haplotypes with positive effects for both mungbean and wheat yield, as well as variants with neutral effects, indicating

207 opportunities to select haplotypes beneficial for system-wide productivity without
208 compromising individual crop performance.

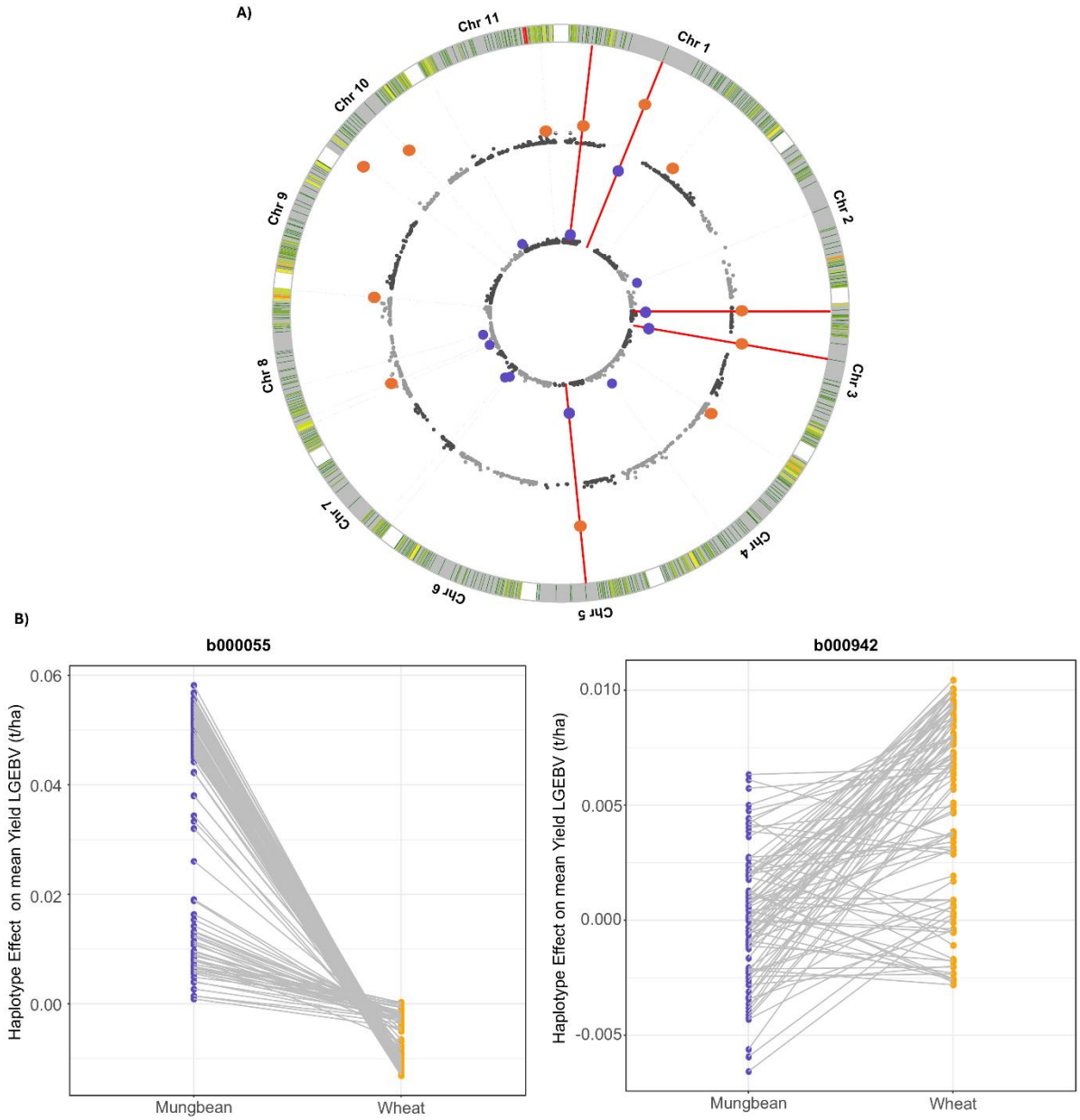

209

210 ***Figure 4. Haploblocks associated with mungbean yield and legacy effects on wheat yield.***
211 *a) Circos plot displaying haploblock effect variance for yield in mungbean (inner ring) and*
212 *wheat (outer ring) following mungbean cultivation. Haploblocks are displayed on the 11*
213 *chromosomes of mungbean. The top 1% of high-variance haploblocks associated with yield*
214 *are highlighted in purple (mungbean) and orange (wheat). Red lines connect shared top*
215 *haploblocks with high haplotype effect variance for yield in both crops, indicating potential*
216 *loci underpinning legacy effects. b) Haplotype effects for mungbean and wheat yield at two*

representative haploblocks: b000055 (chr 1) and b000942 (chr 10). Contrasting or aligned effect directions across species highlight key genomic regions contributing to trade-offs or co-benefits in system-level productivity.

Simulated selection strategies reveal challenges and opportunities for system-level yield optimization

To evaluate the potential for simultaneous genetic improvement of mungbean and its legacy effects on wheat, we simulated haplotype-based selection strategies using variable weighting schemes for the two crops over 25 breeding cycles, using the real haplotype effects as a starting point. Simulated progeny were generated by sampling chromosomes with recombination from selected parents (e.g. Villiers et al, 2022). When haplotypes were selected solely to maximize mungbean yield (100% mungbean weighting), predicted genomic estimated breeding values for mungbean increased by 36.86% over the 25 cycles. However, this improvement came at a cost to the subsequent crop, with legacy wheat yield showing a 7.71% reduction, highlighting the presence of antagonistic haplotypes that benefit mungbean but negatively impact wheat performance within this environment.

Adjusting the selection index to include moderate wheat emphasis (70:30 mungbean:wheat weighting) maintained high genetic gain in mungbean (36.32%) while moderating the negative legacy impact on wheat (reduced to 4.59% loss), demonstrating a more balanced trade-off between direct and legacy benefits. Conversely, placing greater emphasis on wheat legacy performance (30:70 weighting) yielded strong improvements in wheat legacy yield (13.44% increase) with a modest decline in mungbean yield (22.56% reduction), indicating that prioritizing legacy traits can substantially benefit the subsequent crop, albeit at a substantial cost to the legume crop.

Notably, selection based on equal weighting (50:50) resulted in simultaneous yield gains for both mungbean and wheat (19.45% and 7.55%, respectively), though the overall magnitude of improvement was lower than in crop-specific optimization scenarios. This balanced approach highlights the potential of system-wide genetic improvement through integrated breeding strategies that consider both direct performance and legacy effects. The simulation results reveal that while trade-offs exist between optimizing individual crop performance versus rotational benefits, strategic selection can achieve meaningful gains across the entire cropping system, potentially providing a pathway for sustainable intensification through breeding.

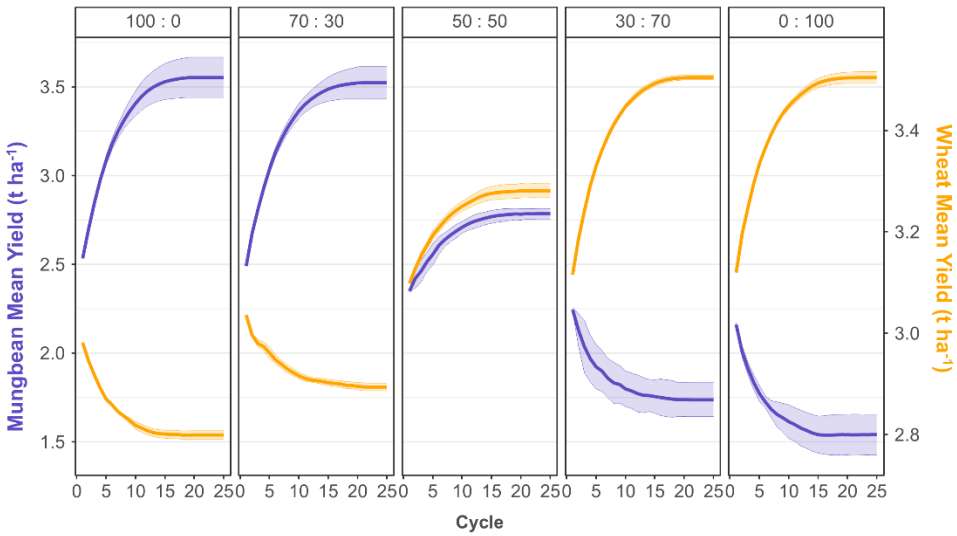

Fig 5. Simulated selection strategies reveal trade-offs and optimistion potential for breeding mungbean with system-level legacy benefits. *Simulations of genomic selection under five haplotype stacking strategies, illustrating their effects on genomic estimated breeding values (GEBVs) for mungbean yield (purple) and legacy wheat yield (orange). From left to right: 100% selection for mungbean yield, 70% mungbean + 30% wheat weighting, equal weighting (50:50), 30% mungbean + 70% wheat weighting, and 100% selection for wheat legacy yield.*

Analysis of soil properties reveals genetic variation for biological drivers of legacy effects

To explore potential traits contributing to legacy effects on subsequent crops, we sampled and analysed soil from a subset of 10 genetically diverse mungbean genotypes after mungbean harvest and prior to wheat sowing. Among the soil nutrient parameters assessed, nitrate (NO_3^-) levels differed significantly between genotypes (p = 0.01), indicating genotype-dependent variation in soil nitrogen dynamics. In contrast, no significant genotypic differences were detected for other soil nutrient components, including ammonium, phosphorus, or exchangeable cations (Supplementary Table 5). To investgate possible differences in soil microbiome due to mungbean genotype, soil volatile components were estimated for the same subset (Supplementary Table 6). Out of a total of 143 volatile organic compounds (VOCs) detected in the soil samples (data not shown), 25 VOCs past the filter criteria of which eleven showed a significant genotypic effect (Supplementary Fig 2). Dehydrocamphor and 2-methylisoborneol showed the largest significant difference among the eleven VOCs with Crystal 8A displaying a significant increase in both VOCs' abundance compared to the bare soil control (Supplementary Fig 3 and Supplementary Table 7). Further, Crystal 8A was

associated with a significantly greater accumulation of dehydrocamphor compared to AusTRC324159 and CPI62672 (Supplementary Fig 3 and Supplementary Table 7). A similar trend follows for 2-pentylfuran, α-fenchyl-methylester, and (5Z)-1-octan-5,7-dienol. However, regarding α-fenchyl-methylester M10452 (Onyx) also displays a significantly higher accumulation compared to bare soil, while (5Z)-1-octa-5,7-dienol was detected at significantly higher levels in AusTRC324159, Celera II AU, Moong, and Crystal 8A compared to bare soil (Supplementary Fig 3 and Supplementary Table 7). Berken displays a distinct soil VOC profile with significantly higher levels of 1,4-*cis*-dimethylcyclooctane, 4,5-dimethylnonane, and 3,7-dimethyloctan-1-ol compared to multiple Mungbean genotypes and the bare soil control (Supplementary Fig 3 and Supplementary Table 7). Interestingly, the potential for Mungbean cultivars to regulate/control the soil microbiome diversity may be best seen in 3-methoxy-3methylbutanol and styrene, where multiple mungbean cultivars are associated with signifcantly reduced accumulation of those VOCs compared to bare soil (Supplementary Fig 3 and Supplementary Table 7).

Discussion

While agricultural research has long demonstrated the value of crop rotations, this study reveals for the first time the potential for rotational benefits to be enhanced through targeted plant breeding by selecting genotypes that shape the environment in ways that influence the performance of subsequent crops. To date, research has focused on species-level benefits (e.g., Li et al., 2019; Lago-Olveira et al., 2023; Salvagiotti et al., 2024), such as nitrogen fixation or disease suppression, rather than legacy variation between genotypes within the initial crop. Our results show that crop legacy effects, defined as the influence of one crop's genotype on the productivity of the next, are under genetic control. In our mungbean–wheat rotation system, substantial phenotypic variation in wheat NDRE, yield and protein content was observed as a function of the preceding mungbean genotype. Importantly, these legacy traits exhibited moderate to high heritability (H^2 = 0.43–0.65), demonstrating that they are amenable to selection. Remarkably, mungbean genotypes enhanced subsequent wheat yield by up to 45% or reduced it by 50% relative to the commercial check variety, revealing substantial genetic variation in legacy effects beyond environmental variation alone. These results highlight a real limitation in traditional breeding that focuses on maximising the performance of a single crop, making an implicit assumption that any effect on subsequent crops is negligible. In contrast, our results demonstrate that legacy effects vary across genotypes and can have a substantial

effect on following crops. This reveals an opportunity for a fundamental shift in breeding philosophy, from exploiting fixed species-level rotational benefits to harnessing genetic variation between species for enhanced system-wide productivity.

Another novel concept demonstrated in this study is that legacy effects can be genetically mapped to the genome of the prior rotation crop. The legacy traits investigated in this case study exhibited complex genetic architecture, where many agronomic traits could have shared genetic control. We identified both shared and unique haploblocks influencing direct mungbean traits and legacy effects on wheat, with 16 high-variance haploblocks showing overlapping effects across both crops. Notably, the magnitude of haplotype effects was consistently greater for mungbean traits than for legacy impacts on wheat, reflecting the range of other factors contributing to wheat performance beyond legacy effects, including the underlying genetics of the wheat cultivar and seasonal growing conditions. Several top haploblocks contained functional genes associated with root development processes, including gibberellin signaling (*MtDELLA2*), root meristem maintenance (*MtPLT1–4*), and auxin transport (*MtPIN2–4*), rather than nodulation-specific pathways. This suggests that some of the legacy traits identified in this study, may be mediated through root growth and architecture, which influence soil nutrient and water status, and rhizosphere interactions, providing a potential mechanistic link between mungbean genotype and subsequent wheat performance.

A trade-off was observed between mungbean yield and its legacy effects on wheat performance, indicating that traits conferring high productivity in one crop may compromise the next crop in rotation. Specifically, high-yielding mungbean genotypes were associated with reduced wheat NDRE at flowering, which in turn was linked to lower wheat yield, consistent with a source–sink limitation driven by environmental modification. This suggests that mungbean genotypes may alter the soil environment through mechanisms such as differential nutrient extraction, altered water availability, or rhizosphere-mediated shifts in the soil microbiome. These changes may reduce resource availability for the subsequent crop, thereby impacting biomass accumulation and final yield. Genomic analysis revealed negative correlations between mungbean haplotype effects on mungbean and wheat traits, with particularly strong trade-offs for yield. For instance, haploblock b000055 showed that haplotypes associated with the highest mungbean yield also had the most detrimental effect on legacy wheat yield, whereas b000942 included haplotypes with neutral or even positive effects on both crops. Importantly, these ‘correlation breakers’ occurred mostly in the lower effect size range, suggesting that system-level improvement may be best achieved through genome-wide strategies like weighted

genomic selection or haplotype stacking, rather than marker-assisted selection for large-effect loci only. Although the precise biological drivers of these legacy effects remain unclear, our targeted soil analyses indicate that there is measurable variation in both nutrient availability and volatile organic compound profiles among a small set of diverse mungbean genotypes (Supplementary Table 5 and 7). It is important to note that while the concept of microbes utilizing VOCs for interkingdom communication is fairly young (i.e. emerging in the last 15 years) soil volatilomic analysis holds enormous potential as a cost-effective means to assess soil health and microbial biodiversity (Weisskopf, et al., 2021). Therefore, while Mungbean genotype-associated manipulations of the soil VOC profile were exposed, the ability to directly link these VOCs to a specific microbe or plant requires additional work outside of the scope of this study. That said, there is promise in the VOCs identified herein. For instance, 2-pentylfuran is known to be emitted from various crops' roots and acts as an attractant for certain insect pests (la Forgia, et al., 2023); 3-methoxy-3-methylbutanol is likely a product of a ligation reaction with the common microbial primary metabolism VOC 3-methylbutanol (Weisskopf et al., 2021); and 2-methylisoborneol and related terpenes (i.e. dehydrocamphor and α-fenchyl-methylester) may indicate the presence of a specific type of bacteria (e.g. actinobacteria, myxobacteria, and cyanobacteria) (Weisskopf et al., 2021; Martin-Sanchez, et al., 2019), This highlights the potential for genotypic influence on the soil environment, potentially via root architecture, nutrient and water acquisition, or microbial community structuring. In particular, legacy effects mediated through persistent changes in the rhizosphere microbiome are a promising avenue, as legume genotypes are known to establish distinct microbial communities that can enhance nutrient cycling and disease suppression for subsequent crops (Yu et al., 2025; Kirkegaard et al., 1997). Together, these findings underscore the need for further biological characterisation of legacy mechanisms and demonstrate the feasibility of incorporating legacy traits into breeding strategies to optimize productivity across crop rotations.

To evaluate the practical implications of these trade-offs, simulated haplotype-based selection strategies revealed clear consequences when breeding solely for single-crop performance within a rotation system. When selection was fully weighted toward mungbean yield, substantial genetic gain in mungbean (36.86%) was observed but consistent reductions in wheat legacy yield (7.71%) were noted, reflecting negative genetic correlations between traits expressed in the two crops. Conversely, selection indices designed to balance genetic gain in both crops moderated these trade-offs when using a 70:30 weighting or even eliminated any tradeoffs in the case of a 50:50 weighting scheme. While absolute genetic gain in each crop

was reduced, overall system performance improved by minimizing negative legacy effects. Most remarkably, equal weighting (50:50) achieved simultaneous yield gains for both mungbean and wheat (19.45% and 7.55%, respectively), demonstrating that direct and legacy traits under negative correlation can be successfully managed through weighted selection indices. In practice, optimal weighting schemes could consider economic factors including relative commodity prices, input costs such as nitrogen fertilizer, and farm-specific production costs, as the economic value of legacy effects may vary substantially depending on market conditions and production systems (Melton et al., 1979). These simulations provide a framework for integrating legacy traits into breeding pipelines, offering insights into how genomic prediction can be optimized to support multi-season, multi-crop production.

The implications of breeding for legacy traits extend far beyond the immediate case study, presenting a promising pathway to enhance agricultural sustainability by reducing input dependency and improving system efficiency. By identifying legume genotypes that promote beneficial downstream effects on cereals, breeders can select varieties that contribute residual nitrogen, improve soil structure, modify soil microbiome, and maintain moisture availability, thereby reducing resource inputs in subsequent crops. This approach can also extend beyond sequential rotations to intercropping systems where genetic variation in root architecture, nitrogen fixation efficiency, and rhizosphere interactions could enhance complementarity and resource-use efficiency. Taking these benefits into consideration, the availability of modern genomic approaches now enable predictive breeding decisions that can harness these potential legacy effects for the first time (Hayes et al., 2024), and the ability to map these effects to defined genomic regions provides a foundation for incorporating them into genomic prediction pipelines. However, implementing this approach at scale requires a paradigm shift that aligns breeding priorities across multiple crops or within large breeding programs that manage multiple crop portfolios simultaneously, as current breeding programs and funding models are structured around single-crop optimization with economic incentives favouring direct trait improvements over legacy effects. Transitioning to legacy trait breeding would require new collaborative frameworks and revised intellectual property models that recognize contributions to farming systems productivity, alongside logistically complex multi-location, multi-season trials to validate genetic effect stability and build industry confidence. Legacy trait expression is likely to exhibit significant genotype-by-environment interactions, particularly when soil properties vary across target production environments, necessitating comprehensive testing to

402 establish breeding value stability. However, this investment in comprehensive testing will be
403 essential to build industry confidence and drive adoption of system-level breeding approaches.

404 As with any trait, studying and improving legacy effects requires sufficient genetic diversity.
405 Elite breeding materials may lack the variation necessary to detect and exploit these effects
406 compared to the mungbean diversity panel used in this research, necessitating the introgression
407 of required genetic variation into breeding populations. This case study also was conducted at
408 a single location with mungbean as the initial crop under nitrogen-deficient, rainfed conditions,
409 which does not fully capture the complexity of legacy dynamics in diverse commercial farming
410 systems. Nonetheless, yield from our mungbean mini-core experiments was similar to that of
411 previous research experiments under different management conditions and years
412 (Supplementary Fig 4). Furthermore, testing legacy effects across multiple wheat genetic
413 backgrounds would reveal whether these effects are consistent across cereal genotypes or if
414 specific legume-cereal genetic combinations maximize rotational benefits. Therefore, future
415 studies involving multi-location trials, diverse cropping systems, and multiple species with
416 appropriate genetic diversity are critical to explore the potential of this approach. Overall, the
417 ability to map legacy effects to defined genomic regions in the initial crop provides a
418 foundation for incorporating these traits into genomic prediction pipelines, enabling more
419 efficient breeding for sustainable farming system outcomes. This work represents a significant
420 advance toward breeding programs that aim to optimize cropping systems rather than a single
421 crop, offering a pathway for improved agricultural sustainability that harnesses genetic
422 diversity to reduce external inputs while maintaining productivity.

423 **Methods**

424 ***Field preparation and site characteristics***

425 Prior to sowing the mungbean panel, soil nitrogen was depleted by sequentially sowing grain
426 sorghum and oat crops to maturity before harvest (Supplementary Fig 5). This depletion
427 addressed the characteristically high nitrogen levels at research farms and created nitrogen-
428 limiting conditions that would maximize expression of genotypic differences in nitrogen
429 fixation capacity and enhance legacy effects on the subsequent wheat crop.

430 ***Plant material and experimental design***

431 A diverse mungbean panel of 309 genotypes was sown on 22nd January 2024 at the Department
432 of Primary Industries research station in Gatton, Australia (27.55 °S; 152.33 °E)
433 (Supplementary Fig 6). This panel consisted of the mungbean mini-core collection, which is a

subset of diverse mungbean germplasm collected from the World Vegetable Center gene bank representing 19 countries across Asia, Australia, Africa and the Americas (Schafleitner et al., 2015). An additional 25 diverse genotypes and one black gram cultivar were included (Supplementary Table 8). The trial used an unbalanced replicated design with the mini-core collection replicated twice and the additional genotypes replicated four times. The experiment was designed using a model-based row-column design incorporating genetic relatedness using the R package 'od' (Cullis et al., 2020).

Mungbean genotypes were sown in 2-row 1.52 m × 4 m plots at a density of 25 plants m^{-2}. Mungbean seeds were inoculated with Group I inoculum (EasyRhiz™, New Edge Microbials Pty. Ltd) at sowing to promote nitrogen fixation through rhizobia establishment in root nodules. Starter fertilizer was applied as a basal application of 25 kg ha^{-1}. When the check cultivar Crystal reached 90% black pod stage, the mungbean trial was desiccated with glyphosate and machine harvested to determine grain yield. The remaining mungbean shoot and stubble was left in the paddock and no tillage occurred prior to planting the wheat trial.

A single wheat cultivar (LongReach Raider) was sown in the same paddock 23 days after harvesting the mungbean trial (23rd May 2024). The wheat was sown in five-row 1.52 m × 4 m plots and a seeding rate of 120 plants m^{-2}, where plot positions overlapped exactly with the previous mungbean plots. Traits measured on the wheat plots were therefore mapped to the corresponding mungbean plot information. Upon maturity, wheat was machine harvested for grain yield determination.

Both trials were conducted under rainfed conditions with appropriate weed, insect and disease control implemented as required. Daily meteorological data (minimum and maximum temperature, rainfall) were obtained from an onsite weather station (Supplementary Fig 7).

Data Collection

A diverse range of agronomic and physiological traits, as well as soil properties, were captured prior and during both mungbean and wheat trials on either the entire trial or on a subset of diverse genotypes (Supplementary Fig 8).

Soil water and nutrient analyses

Prior to the commencement of the mungbean field trial, soil samples were taken from five soil cores across the paddock which were split into two depths (0-20 and 20-40cm) (Supplementary Table 9). These samples were subset into two samples, the first was weighed and dried in 105°C

oven to be weighed again to calculate gravotometic water content (%). A sample of the dried soil was also used for analysis of extractable phosphorus (Colwell P), ammonium nitrogen (NH_4^+), and nitrate nitrogen (NO_3^-) using standard protocols described by Rayment and Lyons (2011). All analyses were performed by an accredited external laboratory using a SEAL AQ400 discrete analyser for colorimetric detection. All final concentrations were converted to mg/kg dry soil for reporting.

Colwell P was extracted using a 0.5 M sodium bicarbonate solution at a 1:50 soil-to-solution ratio. Samples were shaken for 16 hours, centrifuged, and filtered. Phosphorus concentrations in the extracts were determined colorimetrically using the ammonium molybdate–ascorbic acid method, with potassium antimonyl tartrate added to control the reaction rate. Concentrations measured in mg/L were converted to mg/kg based on extraction volume and soil mass.

Ammonium nitrogen (NH_4^+) was extracted using a 2 M potassium chloride (KCl) solution at a 1:10 soil-to-solution ratio and mixed for 1 hour. The resulting extracts were centrifuged and filtered before analysis. Ammonium was quantified colorimetrically through its reaction with sodium salicylate and nitroprusside in a mildly alkaline buffer, forming a coloured complex in the presence of chlorine and detected at 650 nm.

Nitrate nitrogen (NO_3^-) was extracted following the same procedure as ammonium using 2 M KCl. Nitrate was reduced to nitrite via a cadmium reduction column, and the resulting nitrite was measured colorimetrically using a reaction with sulfanilamide and NED, with absorbance read at 540 nm.

Additional soil nutrient analyses were undertaken prior to harvesting the mungbean trial, from two replicates of 10 diverse mungbean genotypes (Supplementary Fig 9; AGG324187 (2B), AusTRC 324159, Berken, Celera II-AU, CHIH-CO, CPI62672, Crystal 8A, M10403, M10452 and Moong). In addition to P, NH_4^+ and NH_3^- being captured, exchangeable bases (Ca, K, Mg, Na) were also measured by using a 1 M ammonium chloride solution at a 1:10 soil-to-solution ratio, shaken for 1 hour. The extracts were centrifuged, filtered, and analysed using a Thermo iCAP PRO XP ICP-OES instrument. Concentrations (mg/L) were converted to mg/kg using extraction volume and soil mass. These values were further converted to milliequivalents (meq/100g) by dividing the mg/kg concentration by the atomic weight of each ion, and then adjusting for charge: divided by 10 for monovalent ions (Na^+, K^+) and by 5 for divalent ions (Ca^{2+}, Mg^{2+}). Cation exchange capacity (CEC) was estimated from the sum of these exchangeable cations.

Soil microbiome analyses

Using a subset of soil samples collected from the ten genotypes described above, soil volatile analyses was undertaken.

HS-SPME-GC/MS analysis

The optimized HS-SPME-GC/MS methodology in Rivers et al. (2019) was modified as follows for the volatilomic analysis of soil samples with the Orbitrap Exploris GC 240 Mass Spectrometer fitted with a TriPlus RSH Multipurpose (i.e. Liquid and Headspace Injection, SPME Arrow, and ITEX-DHS) Extended Rail (Thermo Fisher Scientific, Massachusetts, USA). Splitless mode on the was employed for application of the VOCs via a 1.0mm straight no-wool liner to a TRACE 1610 series Gas Chromatograph (Thermo Fisher Scientific). Soil samples, QC samples, laboratory blanks, and standards were block randomised throughout each batch. Each sample was place on 2ml of 20% NaCl solution and incubated at 80ºC for 40 min with continuous agitation at 500 rpm for enhance VOC volatilization and homogenization. VOC extraction (adsorption) was carried out by exposing a broad specificity SPME Arrow fibre (1.10mm DVB/C-WR/PDMS 110µm x 20mm, Thermo Fisher Scientific) to soil sample head space for 40 min with continuous agitation at 1000 rpm. Extracted VOCs underwent desorption from the SPME Arrow on to the GC column (TraceGOLD TG-5SilMS GC Column, Thermo Fisher Scientific) via the inlet at 250ºC for 10 min. Between samples the SPME Arrow fibre undergoes a pre- and post-conditioning at 250ºC for an additional 10 min to prevent cross sample contamination. Chromatographic separation of the soil VOCs was achieved employing ultra-pure Helium as a carrier gas and via a 38.5 min oven temperature program: 40ºC for 2 mins, increasing to 150ºC at a ramp rate of 5ºC /min and held for 2 min, and then increased to 320ºC at 15ºC/min and held for 1 min. Lastly, the Orbitrap Exploris 240 MS was operated in full MS scan acquisition using electron ionisation at 70eV from m/z 40-500 with a lag time of 5min, and a Orbitrap resolution of 60,000. Temperatures were 320oC for the Auxillary transfer line and 250oC for the ion source.

Volatile Data Analysis

Thermo Compound Discoverer (ver. 3.3.2.31) was used for deconvolution and data analysis. The NIST/EPA/NIH Mass spectral libraries (ver. 2023) were used for mass spectral matching and peak annotations. Using an *n*-alkanes (C7-C40) standard mix Kovats non-isothermal retention indices (RIs) were calculated and compared to reference semistandard non-polar RIs from the NIST and Pubchem databases when available. Peak intensity values were collected

529 and corrected based on the internal standard nitrobenzene, background peak detection in blank
530 samples, and sample weight. Subsequent statistical analyses were carried out using
531 MetaboAnalyst 6.0 (www.metaboanalyst.ca).

532 *Total aboveground biomass*

533 In the mungbean trial, biomass samples were harvested from 1-4 replications of a subset of 47
534 diverse lines. Sampling occurred when the commercial check cultivar Crystal reached
535 flowering (50% of the plot had open flower), which represented mid canopy development.
536 Samples were taken from 0.5 x 1.52 m of the two rows per plot. For the wheat trial, biomass
537 cuts were taken from the same plots as the preceeding mungbean trial at heading. Samples were
538 harvested from 0.5 x 0.75 m of the two middle rows per plot and dried at 65°C for 5 days
539 before weighing for total biomass.

540 *Vegeatation indices*

541 Vegetation indices were extracted from a multispectral sensor mounted on an unmanned aerial
542 vehicle platform flown across the mungbean trial when check cultivar Crystal was at the
543 flowering and 90% black pod growth stages. The UAV imagery approach for mungbean is
544 described in detail in Van Haeften et al (2025). Briefly, a MicaSense Altum™ sensor
545 (MicaSense Inc., Seattle, Washington, USA) was flown onboard a Matrice 300 RTK (DJI,
546 USA) UAV platform. Appropriate flight conditions and calibrations were maintained for each
547 flight to ensure high-quality image capture. Images were stitched to generate georeferenced
548 orthomosaics and digital surface models using Pix4D software. Plot boundaries were defined
549 in ArcMap for the mungbean trial and applied to the wheat trial to ensure corresponding wheat
550 plots aligned with previous mungbean genotype plots. Normalized difference red edge index
551 (NDRE), height, thermal and canopy coverage were extracted using orthomosaics, digital
552 surface models, and shape files in a Python environment-based program developed at The
553 University of Queensland (Das et al., 2022). These traits were used to estimate aboveground
554 biomass in mungbean during mid-canopy development (determined when Crystal had reached
555 50% flowering), as described in the 'mungbean biomass prediction models' section below. In
556 addition, raw NDRE values were extracted for analysis at 90% black pod stage in mungbean
557 and at flowering in the subsequent wheat crop.

558 *Grain quality characteristics*

559 Wheat grain protein content was measured using near-infrared spectroscopy with an Inframatic
560 9500 (IM9500) Grain Analyser (Perten Instruments). The instrument warmed up for a

minimum of 30 minutes and self-calibrated using the internal reference standard per manufacturer recommendations. Approximately 200 g sub-samples were loaded into the IM9500 sample hopper for analysis. The IM9500 conducted three sub-sample readings and averaged spectra before predicting constituent values. Each sample was analysed in triplicate; between replicates, the hopper was emptied and refilled with fresh sample portions. Protein content was reported on a 12% moisture basis.

Statistical Analyses

Mungbean biomass prediction models

Mungbean biomass predictions used the UAV flight corresponding to mid-canopy development which was determined by flowering time for check cultivar Crystal and ground-based biomass measurements collected on the same day. This stage represented mid-canopy development, and a prediction model previously developed for mungbean at this stage (Van Haeften et al., 2025) was applied. This stepwise regression model incorporated height, thermal, NDRE and coverage. Model validation used an 80/20 training/testing split.

Single-site spatial analyses

Single site spatial analysis accounted for spatial variation across the site for all traits. Both fixed and random row and column terms were tested for model improvement and retained as needed. Wald statistics determined significance of fixed effects, whilst AIC, BIC and Log-likelihood assessed model fit changes due to added random components. Best Linear Unbiased Estimators (BLUEs) and Best Linear Unbiased Predictors (BLUPs) were calculated using equation 1:

$$y = Xb + Zu + e \tag{1}$$

where b is a vector of fixed effects, Z is a vector of random effects, X and Z are the associated design matrices and e is the residual.

Generalised broad sense heritability for each trait was calculated per Cullis et al (2006) using equation 2:

$$H_g^2 = 1 - \frac{A_{tt}}{(2\gamma_v)} \tag{2}$$

where A_{tt} is the average prediction error variance and γ_v is the genetic variance estimated by the model.

590 ***Correlations***

591 Phenotypic correlations between traits were calculated using Pearson's correlation coefficient
592 based on BLUEs for each genotype. Statistical significance was assessed using two-tailed p-
593 values, with non-significant correlations ($p > 0.05$) flagged in visualisations. The same
594 methodology calculated correlations between haplotype variances and haplotype effects.

595 Genetic correlations were calculated for each trait pair using mixed linear models with
596 unstructured variance structures applied to trait-to-trait interaction terms as per equation 3:

597 $$\begin{bmatrix} y_1 \\ y_2 \end{bmatrix} = \begin{bmatrix} X_1 & 0 \\ 0 & X_2 \end{bmatrix} \begin{bmatrix} \beta_1 \\ \beta_2 \end{bmatrix} + \begin{bmatrix} Z_1 & 0 \\ 0 & Z_2 \end{bmatrix} \begin{bmatrix} u_1 \\ u_2 \end{bmatrix} + \begin{bmatrix} \varepsilon_1 \\ \varepsilon_2 \end{bmatrix} \quad (3)$$

598 where y represents phenotype vectors for traits 1 and 2 respectively, X and Z are design
599 matrices for the fixed and random components of the model, β represents coefficient of fixed
600 effects, u represents the random genetic effects, and ε is the residual. Covariance between
601 genetic effects is represented as $Var(u) = G \otimes K$, where K is the genomic relationship matrix
602 (GRM) and G is the genetic covariance matrix between traits.

603 ***Genomic analyses***

604 DArTseq markers were curated based on a minor allele frequency greater then 0.05,
605 heterozygosity of less then 0.2, and <20% missing calls, resulting in 5,516 high quality
606 markers. Linkage disequilibrium was explored to identify suitable thresholds for haploblock
607 definition. The R package 'Selection Tools' defined haploblocks with markers in LD >0.3 and
608 a marker tolerance of 4. Marker tolerance represents the maximum number of markers that can
609 be skipped during haploblock creation, chosen based on the potential for misalignment. This
610 approach defined 1,126 haploblocks with an average of 4.9 markers per block.

611 Marker effects were calculated using ridge-regression BLUP to determine simultaneous effects
612 of all SNPs per equation 4.

613 $$y = WGu + \varepsilon \quad (4)$$

614 where u is a vector of marker effects, G is the genotype matrix, W is a design matrix relating
615 genotypes to observations (y), and ε is the error. Relevant SNP effects were summed to
616 calculate haplotype effects at each haploblock. Effect variance was calculated, with the top 1%
617 of haploblocks by variance (rounded up to 12) selected for each trait and considered to be a
618 related block for that trait.

Identifying and co-locating mungbean othologues for functional legume genes

Minimap2 (Li, 2018) was used to extract regions corresponding to identified haploblocks in a Crystal reference genome enhanced with additional PacBio HiFi long-read sequencing data (Mens & Udvardi, unpublished). Mungbean orthologues of known nodulation and nitrogen fixation genes were identified using reciprocal tBLASTn searches (E-value threshold ≤ 1e-5) against a compiled list of over 200 characterised genes in model legume systems (Roy et al., 2022). Orthologues were retained if overlapping with atleast one of the five haploblocks.

Weighted selection strategies simulations

Three mungbean breeding programs targeting genetic improvement were simulated: 1) mungbean yield alone, 2) legacy wheat yield alone, and 3) simultaneous improvement of both. For simultaneous improvement, selection used trait indices calculated as weighted sums of breeding values with weights of 0.7:0.3, 0.5:0.5, and 0.3:0.7 for mungbean:wheat yield, respectively. Simulations used SNP effects estimated from genomic prediction models to calculate genomic estimated breeding values (GEBVs). Each program ran 25 cycles, selecting 30 parents per cycle based on program-specific criteria. Selected parents were randomly mated to create 50 crosses, with 100 progenies per cross, generating 5000 selection candidates for the next cycle. Genetic improvement was assessed by population mean GEBV changes per cycle. Each program was simulated five times, reporting average values and 95% confidence intervals of population mean GEBVs using the genomicSimulation R package (Villiers et al., 2022).

Comparison of genotypic differences for soil characteristics

To evaluate whether soil characteristics differed significantly among the subset of 10 diverse mungbean genotypes, a one-way analysis of variance (ANOVA) was performed for each measured soil variable. Genotype was treated as a fixed effect, and significance was assessed to determine whether plant genetic variation contributed to differences in soil nutrient concentrations and moisture content.

Acknowledgments

We thank the World Vegetable Center (WorldVeg), particularly Roland Schafleitner and Ram Nair, for providing the genomic data for the mungbean mini core collection that formed the foundation of this study. We are grateful to Queensland Department of Primary Industries for Gatton field trial support, and provision of the Hermitage 2018 yield datasets. We particularly acknowledge the technical staff at the Gatton Research Facility for their assistance with field operations, and trial management. We thank LongReach Plant Breeders for generating the wheat grain protein data.

Data availability

All primary data supporting the findings of this study are available via The University of Queensland eSpace repository at https://doi.org/10.48610/cee8b66.

Funding

This work was supported by The University of Queensland start-up funds awarded to MS. Mungbean research to MS, LH, MU at The University of Queensland was supported by the Australian Centre for International Agricultural Research International Mungbean Improvement Network Phase 2 (CIM2014/079) and Grains Research & Development Corporation Genetic Initiative to Transform Symbiotic Nitrogen Fixation in Australian Pulse Crops (UOQ2403-012RTX) .LH was supported through an ARC Future Fellowship (FT220100350). ED is supported by the Queensland Government's Industry Research Fellowships program (AQIRF096-2023RD6). SVH, ME were recipients Grains Research & Development Corporation Research Scholarship (UOQ2101-003RSX; UOQ2410-011RSX). SVH, SMB were recipients of an Australian Government Research Training Program Scholarship. SMB was supported as a PhD student by the Deutsche Forschungsgemeinschaft (DFG) and University of Queensland International Research Training Group 2843 – Accelerating Crop Genetic Gain. ME was supported as a PhD student of the Australian Research Council Training Centre in Predictive Breeding for Agricultural Futures (IC230100016).

Authors contributions

Shanice Van Haeften: Writing – Original Draft Preparation, Investigation, Data Curation, Formal analyses, Visualisation. **Stephanie Brunner:** Writing – Original Draft Preparation, Data Curation, Formal analyses, Visualisation. **Eric Dingalsan:** Methodology, Writing – Review & Editing. **Edward Fabreag:** Formal analyses, Writing – Review & Editing. **Joseph**

Eyre: Methodology, Investigation, Writing – Review & Editing. **Celine Mens:** Investigation**.** **Ben J. Hayes:** Supervision, Writing – Review & Editing. **Michael Udvardi:** Supervision**,** Writing – Review & Editing. **Samir Alahmad:** Investigation. **Mitchell Eglinton:** Investigation, Writing – Review & Editing. **Ryan McQuinn:** Investigation, Formal analyses, Writing – Review & Editing. **Merril Ryan**: Resources, Writing – Review & Editing. **Sarah van der Meer:** Investigation. **Millicent R. Smith:** Conceptualisation**, Funding Acquisition, Project Administration,** Writing – Review & Editing. **Lee T. Hickey:** Conceptualisation , **Project Administration** Writing – Review & Editing.

Competing interests

The authors declare no competing interests.

References

Bennett, A. J., Bending, G. D., Chandler, D., Hilton, S. & Mills, P. Meeting the demand for crop production: the challenge of yield decline in crops grown in short rotations. Biol. Rev. 87, 52–71 (2012).

Cernay, C., Makowski, D. & Pelzer, E. Preceding cultivation of grain legumes increases cereal yields under low nitrogen input conditions. Environ. Chem. Lett. 16, 631–636 (2018).

Ellouze, W. et al. Chickpea genotypes shape the soil microbiome and affect the establishment of the subsequent durum wheat crop in the semiarid North American Great Plains. Soil Biol. Biochem. 63, 129–141 (2013).

Evenson, R. E. & Gollin, D. Assessing the impact of the Green Revolution, 1960 to 2000. Science 300, 758–762 (2003).

Foyer, C. H., Nguyen, H. & Lam, H. M. Legumes—the art and science of environmentally sustainable agriculture. Plant Cell Environ. 42, 1–5 (2019).

Hayes, B. J. et al. Potential approaches to create ultimate genotypes in crops and livestock. Nat. Genet. 56, 2310–2317 (2024).

Hickey, L. T. et al. Breeding crops to feed 10 billion. Nat. Biotechnol. 37, 744–754 (2019).

Ilyas, N. et al. Contribution of nitrogen fixed by mung bean to the following wheat crop. Commun. Soil Sci. Plant Anal. 49, 148–158 (2018).

Kirkegaard, J. A., Hocking, P. J., Angus, J. F., Howe, G. N. & Gardner, P. A. Comparison of canola, Indian mustard and Linola in two contrasting environments. II. Break-crop and nitrogen effects on subsequent wheat crops. Field Crops Res. 52, 179–191 (1997).

La Forgia, D., Martin, C., Turlings, T. C. & Verheggen, F. 2-Pentylfuran: an aggregation attractant for wireworms. Arthropod-Plant Interact. 17, 465–472 (2023).

Lago-Olveira, S., Rebolledo-Leiva, R., Garofalo, P., Moreira, M. T. & González-García, S. Environmental and economic benefits of wheat and chickpea crop rotation in the Mediterranean region of Apulia (Italy). Sci. Total Environ. 896, 165124 (2023).

Li, J. et al. Diversifying crop rotation improves system robustness. Agron. Sustain. Dev. 39, 38 (2019).

Li, L., Awada, T., Shi, Y., Jin, V. L. & Kaiser, M. Global greenhouse gas emissions from agriculture: pathways to sustainable reductions. Glob. Change Biol. 31, e70015 (2025).

Lilley, J. M. & Kirkegaard, J. A. Farming system context drives the value of deep wheat roots in semi-arid environments. J. Exp. Bot. 67, 3665–3681 (2016).

Martín-Sánchez, L. et al. Phylogenomic analyses and distribution of terpene synthases among Streptomyces. Beilstein J. Org. Chem. 15, 1181–1193 (2019).

Melton, B. E., Heady, E. O. & Willham, R. L. Estimation of economic values for selection indices. Anim. Sci. 28, 279–286 (1979).

Rivers, J. Y., Truong, T. T., Pogson, B. J. & McQuinn, R. P. Volatile apocarotenoid discovery and quantification in Arabidopsis thaliana: optimized sensitive analysis via HS-SPME-GC/MS. Metabolomics 15, 79 (2019).

Rose, T. J., Damon, P. & Rengel, Z. Phosphorus-efficient faba bean (Vicia faba L.) genotypes enhance subsequent wheat crop growth in an acid and an alkaline soil. Crop Pasture Sci. 61, 1009–1016 (2010).

Salvagiotti, F., Biassoni, M. M., Magnano, L. & Bacigaluppo, S. Enhanced seed yield of full-season soybean when rotated with cereals and cover crops as compared to monoculture in a long-term experiment. Eur. J. Agron. 161, 127382 (2024).

Somenahally, A. et al. Microbial communities in soil profile are more responsive to legacy effects of wheat-cover crop rotations than tillage systems. Soil Biol. Biochem. 123, 126–135 (2018).

Villiers, K., Dinglasan, E., Hayes, B. J. & Voss-Fels, K. P. genomicSimulation: fast R functions for stochastic simulation of breeding programs. G3 12, jkac216 (2022).

Voss-Fels, K. P., Cooper, M. & Hayes, B. J. Accelerating crop genetic gains with genomic selection. Theor. Appl. Genet. 132, 669–686 (2019).

Weisskopf, L., Schulz, S. & Garbeva, P. Microbial volatile organic compounds in intra-kingdom and inter-kingdom interactions. Nat. Rev. Microbiol. 19, 391–404 (2021).

Yu, S., Wang, T., Wang, L., Yao, S. & Zhang, B. Preceding crop rotation systems shape the selection process of wheat root-associated bacterial communities. J. Integr. Agric. 24, 739–753 (2025).

Zhao, J. et al. Global systematic review with meta-analysis reveals yield advantage of legume-based rotations and its drivers. Nat. Commun. 13, 4926 (2022).